

Real-Time Data Muling using a team of heterogeneous unmanned aerial vehicles

Emmanuel Tuyishimire¹, Antoine Bagula¹, Slim Rekhis², Nouredine Boudriga²

¹ *Computer Science Department, University of the Western Cape, Cape Town, South Africa*

² *Communication Networks and Security Research Laboratory, Carthage University, Tunis, Tunisia*

Abstract

The use of Unmanned Aerial Vehicles (UAVs) in Data transport has attracted a lot of attention and applications, as a modern traffic engineering technique used in data sensing, transport, and delivery to where infrastructure is available for its interpretation. Due to UAVs constraints such as limited power lifetime, it has been necessary to assist them with ground sensors to gather local data which has to be transferred to UAVs upon visiting the sensors. The management of such ground sensor communication together with a team of flying UAVs constitutes an interesting data muling problem which still deserves to be addressed and investigated. This paper revisits the issue of traffic engineering in Internet-of-Things (IoT) settings, to assess the relevance of using UAVs for the persistent collection of sensor readings from the sensor nodes located into an environment and their delivery to base stations where further processing is performed. We propose a persistent path planning and UAV allocation model, where a team of heterogeneous UAVs coming from various base stations are used to collect data from ground sensors and deliver the collected information to their closest base stations. This problem is mathematically formalised as a real-time constrained optimisation model, and proven to be NP-hard. The paper proposes a heuristic solution to the problem and evaluates its relative efficiency through performing experiments on both artificial and real sensors networks, using various scenarios of UAVs settings.

Keywords: Real-time visitation, cooperative UAVs, path planing, clustered network.

1. Introduction

The use of UAVs has emerged as a flexible and cost-efficient alternative to traditional traffic engineering techniques which have been used in IoT settings, to transport sensor readings from their points of collection to their processing places. However, the joint path finding and resource allocation for a team when

tasked to achieve collaborative data muling, is still an issue that require further investigations. On the other hand, while accurate solutions to data muling problems are still scarce, especially when considering the limited flying capacity of the battery-powered UAVs, issues related to the efficient task allocation to a team of UAVs under stringent data collection requirements, such as real time data collection, still need to be addressed, especially when UAVs have different specifications (speeds, battery, lifetime, memory, functionalities, etc) and only fresh and complete information need to be collected. Furthermore, persistent collection requirement needs to be addressed and this requires the data muling system to deal with outdated or premature sensor readings.

Potential applications of a such real-time data muling model include (i) city surveillance in order to evaluate risks and respond with appropriate actions by having a team of UAVs persistently visiting locations of interests in a smart city for public safety, parking spots localization [1] and pollution monitoring [2] ; (ii) drought mitigation to support small scale farming in rural areas [3, 4] by using a team of UAVs to collect farmland image collection and processing these images to achieve situation recognition for precision irrigation; (iii) periodic surveillance of buildings and cities' infrastructures for structural health monitoring and maintenance; and (iv) extension of the reach of community mesh networks in rural settings for healthcare [5, 6] by using a team of UAVs (such as drones) as wireless access points.

Sensors visitation under the fuel consumption constraints was addressed in [7], and the visitation under the revisit deadline constraint was proposed in [8]. Both works assumed a single moving agent (UAV) which optimally visits various targets. [9] proposes a cooperative UAVs model where many targets are visited by a team of UAVs for persistent surveillance and pursuit. In this work, the UAVs do not communicate with each other but rather rely on the information from the static underground sensors, which are optimally placed as proposed in [10]. However, all these models do not consider the persistent data delivery and heterogeneity of UAVs which might have different fabrics and characteristics. Furthermore, neither the energy/battery consumption while the UAVs are waiting for the updated information from the terrestrial sensor network nor the penalty associated with stale information due to late visitation by the UAV to the sensor nodes have been accounted for. While models were proposed in [11, 12, 13, 14] for the periodic and persistent UAVs visitation of a single target from different positions, the models do not consider the path planning issues which are as necessary as the path planning especially for restricted environments. Multiple UAVs models have also been employed to visit many target [15, 16, 17, 18]. Here the focus was the efficient target visitation and the assignment issue has not been addressed. However when heterogeneous UAVs have to visit multiple sensors, an UAVs assignment model is required to complement path planning models.

This paper assumes a restricted and complex network, where sensors are not only connected in terms of their ability to forward data to each other, but also in terms of the possible paths UAVs may use to visit each sensor from any base station or any other sensor in a region of interest. We propose a

persistent and real-time path planning together with a task allocation model where, a team of heterogeneous UAVs coming from various base stations are used to collect sensor readings from ground sensors and deliver the collected information to their closest base stations. The underlying data muling problem is i) mathematically formalised as a real-time constrained optimisation problem, ii) proven to be intractable and iii) solved using a novel heuristic solution, whose relative efficiency is proven through running experiments on both artificial and real sensor network, with various UAVs settings.

This paper is an extension of the work in [19]. An extension has been done by detailing the work and the proposed model has been transformed to make the model real-time respondent. Furthermore, analysis results corresponding to added features have been provided.

The rest of this paper is organised as follows. The cooperative data muling model is presented in Section 2 and its algorithmic solution provided in the same section. Simulated results are provided and discussed in Section 3 while the conclusion is drawn in Section 4.

2. The Cooperative Data Muling Model

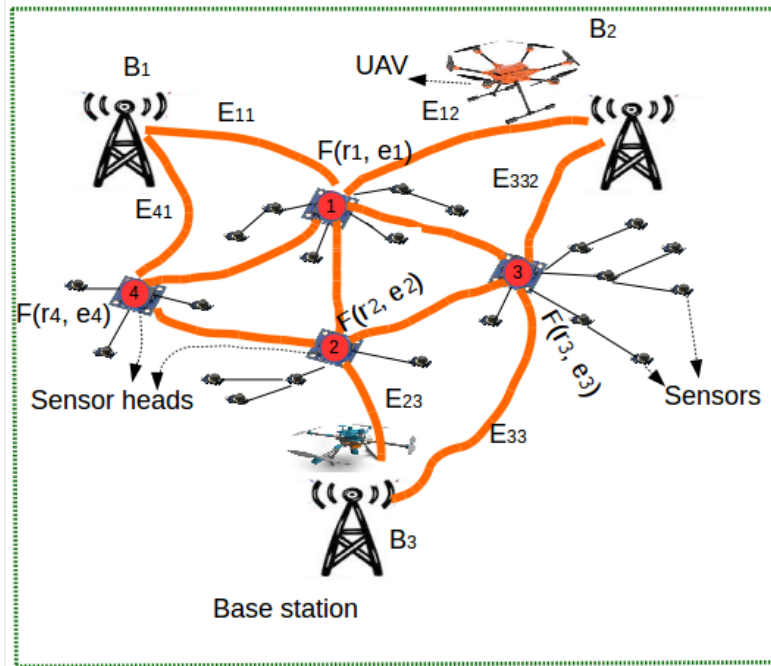


Figure 1: Cooperative Data Muling

In this paper, we consider an “Internet-of-Things in Motion” model as shown in Figure 1. We assume that UAVs are assisted by special ground-based sensors

which locally collect data from other sensors. That is, sensors are grouped into separated clusters, each with its own sink node (the cluster head), where the information is to be collected from other sensor nodes (cluster members) and relayed to UAVs which deliver the sensor readings to base stations. Note that only cluster heads can communicate with UAVs, and the optimal clustering scheme is not covered in this paper. Furthermore, the inner cluster communication technology is not covered here (it has been discussed in [20, 21, 22]).

The cooperative data muling model considered in this paper is illustrated by Figure 1. The figure reveals three base stations (B_1 , B_2 and B_3) from where UAVs take off to collect data from sinks located in a region of interest and later comes back for data delivery. In this illustrative scenario, all possible collection paths which can be taken by each UAV from the base stations to access data collected by cluster heads (1, 2, 3 and 4) and deliver the collected data to the closest base stations, are represented in big and orange lines. Here, we assume that UAVs are assisted by special nodes (cluster heads/sinks) to collect information to reduce the loss due to UAVs capabilities (fuelling, timing, etc.). Furthermore, it is assumed that the UAVs paths topology is known (this means that all possible communication paths between all sensors are known) and it is represented by small black lines in the figure. The total energy required for data collection at a node/sensor, say i , is a function $F(r_i, e_i)$ of its revisit deadline r_i (the maximum amount of time required to (re)visit the node) and the energy e_i required to transfer data from node i to an arriving UAV. The travel cost from a base station B_j to a sink i is translated in an energy metric denoted by E_{ij} , and the transportation cost between two sinks i and k is also translated into an energy metric denoted by e_{ik} .

2.1. The Data Muling Problem

In this subsection, the problem is modelled as a constrained optimisation problem. We start by defining/denoting all cost related terms and later, we combine them to form a cost function.

2.1.1. UAVs waiting time on sink nodes

Let t_i be the entire time spent by an UAV to arrive at the sink i since it took off from a base station and r_i be the expected time for a UAV to arrive at the sink i . It is also referred to as *revisit time* at the collection point i .

The sink visitation-based cost may be expressed in terms of penalties for both early and late visits on the sink nodes, the collection of information and a risk associated with the autonomy of the UAVs. These costs are described as follows.

- **Early visit penalty:** An early visit penalty will be assigned to an UAV if $t_i < r_i$ to express the case where the visiting UAV arrive premature data collection. In this case, the UAV will wait for a period of time $w_i = r_i - t_i$ needed by the sink node to capture mature information from the field and transmit it to the waiting UAV.

- **Late visit penalty:** A late visit penalty will be applied to the UAV if $t_i > r_i$ to express the fact that the visiting UAV is late by a period of time $l_i = t_i - r_i$ wasted by the UAV to arrive late to a collection point where data was ready for collection. This penalty can also be expressed using a piece-wise function.
- **Data collection cost:** A data collection cost will be applied to any UAV to consider the fact that the UAV has to use the energy e_i to collect information from the visited node i . Note that while the costs w_i and l_i depend on how the terrestrial and airborne sink networks have been traffic engineered, the data collection cost e_i may depend on different engineering parameters and functions which may be bound to the communication interfaces of the equipment used by both the ground sink nodes and the UAVs and the protocol used for such communication.

For each UAV, the total cost $F(r, e_i)$ of visiting the sink i , without taking into account the travelling cost is expressed by

$$F(r_i, e_i) = \alpha w_i u(w_i) + \beta l_i u(l_i) + \gamma e_i, \quad (1)$$

where $u(w_i)$ and $u(l_i)$ are the values of a unit step function applied to w_i and l_i , respectively. The coefficients α , β , and γ are associated with the setting-based importance/weighting allocated to the early and late arrival penalties and the data transfer penalty respectively.

2.1.2. The assumed network

We consider a hybrid sensor network (a network with multiple types of links) that represented by a bi-directed graph $\mathcal{G} = (\mathcal{S}, \mathcal{N}, \mathcal{L}, \mathcal{B}, \mathcal{P})$, where \mathcal{S} is the set of all sensor nodes, $\mathcal{N} \subset \mathcal{S}$ is the set of all sinks, \mathcal{L} is the set of wireless communication links between the sensor nodes, \mathcal{B} is the set of UAV base stations while \mathcal{P} is the set links showing possible moves of UAVs. Here, a move expresses one of the two following kinds of connection.

- **Base station-sink :** These are bidirectional UAVs paths connecting sinks and base stations. The cost of moving from a base station b to a sink i is denoted E_{bi} and its opposite is E_{ib} , with $E_{ib} = E_{bi}$.
- **sink-sink :** These are the UAVs paths connecting sinks amongst themselves and the cost to move from one sink i to j is denoted by e_{ij} , with $e_{ij} = e_{ji}$.

2.1.3. Initial condition

- Each UAV is assumed to start its journey from a base station.
- The waiting times at all sensor nodes. That is $l_i = w_j = 0, \forall i, j \in \mathcal{N}$

Here, it is assumed that the maximum number of UAVs at each base station is equal to the degree/capacity of the base station.

2.1.4. The data muling modelling

The data muling is performed in two steps

- **Data collection.** During data collection, an UAV is to move from a Base station a to collect data from $k > 0$ sinks labelled by a set of indices $p^* = [1, 2, \dots, k]$. In this case, we represent the path used for data collection by $p = [a, 1, 2, \dots, k]$. The energy required for this step is expressed by

$$C(p) = E_{a1} + \sum_{i \in p^*} F(r_i, e_i) + \sum_{i, j \in p^* \wedge j=i+1} e_{ij}. \quad (2)$$

- **Data delivery.** During data delivery, a UAV may or many not pass by some already visited sink to deliver information to closest base station b . However, the end point of the collection path p is the starting point of the delivery path. In this case, the corresponding energy is expressed as a function $E(p)$ of the data collection path.

Therefore, the total energy required for data collection and delivery is given by the equation

$$C(p) + E(p) = E_{a1} + \sum_{i \in p^*} F(r_i, e_i) + \sum_{i, j \in p^* \wedge j=i+1} (e_{ij}) + E(p). \quad (3)$$

The data muling problem consists of finding for each UAV an optimal path so that the total energy spent by all the UAVs to collect and deliver the sensor readings/data without colliding is minimized. Mathematically, we represent the set of UAVs by $U = \{1, 2, 3, \dots, m\}$, where each UAV say u departing from base station a_u will follow path p_u to collect data at locations of interest and another path (maybe different from p_u) to deliver the data to its closet base station. Let's consider 1_u , the first sink to be visited by the UAV u . The data muling problem is formulated as follows.

$$\min Z = \sum_{u=1}^m \left(E_{a_u 1_u} + \sum_{i \in p_u^*} F(r_i, e_i) + \sum_{\substack{i, j \in p_u^* \\ j=i+1}} (e_{ij}) + E(p_u) \right), \quad (4)$$

subject to

$$(4.1) \quad \forall v, w \in U, p_v^* \cap p_w^* = \emptyset = d(p_v^*) \cap d(p_w^*)$$

$$(4.2) \quad \bigcup_{u \in U} p_u^* = S$$

$$(4.3) \quad e_i, e_{ij}, E(p), r, E_{a_u 1_u} \geq 0, \forall i, j, p, a_u, 1_u.$$

Here, the first constraint states that any two collection or delivery paths have no sink in common. This guarantees collision avoidance for the UAVs. On the other hand, the second constraint expresses the fact that all sinks are to be visited.

2.2. Real-time visitation

We consider Equation 1. In the scenarios where the variables have very strict conditions, instead of being part of the cost function, they need to be part of the problem constraints. Table 1 shows all possible models. Here a "1" shows the case where a corresponding variable is restricted (part of the constraints) and a "0" shows the other way.

Waiting penalty (w_i)	Late penalty (l_i)	Explanation
0	0	None of the two variables is bounded
0	1	Only the late penalty is bounded
1	0	Only the waiting penalty is bounded
1	1	Both variables are bounded

Table 1: Data collection scenarios.

The optimisation problem changes its constraints so as to become as follows.

$$\min Z = \sum_{u=1}^m \left(E_{a_u 1_u} + \sum_{i \in p_u^*} F(r_i, e_i) + \sum_{\substack{i, j \in p_u^* \\ j=i+1}} (e_{ij}) + E(p_u) \right), \quad (5)$$

subject to

$$(5.1) \quad \forall v, w \in U, p_v^* \cap p_w^* = \emptyset = d(p_v^*) \cap d(p_w^*)$$

$$(5.2) \quad \bigcup_{u \in U} p_u^* = S$$

$$(5.3) \quad 0 \leq w_i \leq W_i$$

$$(5.4) \quad 0 \leq l_i \leq L_i$$

$$(5.5) \quad e_i, e_{ij}, E(p), r, E_{a_u 1_u} \geq 0, \forall i, j, p, a_u, 1_u.$$

where W_i and L_i are the predetermined thresholds which may take any non negative value.

2.3. Related problems and solutions

The data muling problem considered in this paper is closely related to the file recovery problem in [23] (NP-hard problem) solved by curving techniques, including those using the Parallel Unique Path (PUP) algorithm. This problem considers a case of many fragmented files which need to be reassembled, starting from their headers, which are assumed to be known initially. The PUP algorithm is a variation of Dijkstra's routing algorithm[24] where starting from the headers, clusters are successively added based on their best matches. This is done with the aim of building paths from headers having a cluster added to an existing path if and only if the link to it has the least weight. On the other hand the Vehicle Routing Problem (VRP)[25, 26] consists of finding the optimal road from a depot, to be taken for delivering resources to customers and return to the depot. Exact and heuristic algorithms for its solution have been surveyed in[25]. In the survey, all stated algorithms assume a single distance matrix (the cost matrix) and hence could fail to be a good fit for our persistent visitation scenario since in our case the weighting of nodes matters and it is not a fixed value. Furthermore, for the VRP, vehicles end their trips at the depots where they started from. This would limit the number of topologies where the data muling problem is solvable and also could impose a data muling scheme which is not necessarily optimal. Note that in our case, we are interested in the case where the late and stale visitation are taken care of, and this depends on the dynamic position of UAVs (see the Equation 1). Furthermore, UAVs deliver the collected information to optimal base stations (which are not necessarily their starting points).

2.4. The data muling problem intractability

To prove its intractability, we provide a polynomial reduction of one-depot VRP (which is known to be an NP-hard problem), into a special case of the data muling problem: the case where each sink's weight is zero. The transformation consists of a two-step process which transforms the graph \mathcal{G} as follows.

- a. Group all Base stations in \mathcal{S} in one cluster/group and consider this cluster/group as a special node for the graph, this gives the VRP's topology $\mathcal{G}' = (\mathcal{S}, \mathcal{N}, \mathcal{L}, \mathcal{B}', \mathcal{P})$, where $\#\mathcal{B}' = 1$.
- b. For every link of \mathcal{G}' , make the link weight in the new graph (found in a.) the inverse of the weight in the Graph \mathcal{G}' .

This will reduce the VRP's into the data muling problem's solution.

Clearly, the time complexity of the transformation process is polynomial since Step *a* has a complexity $\mathcal{O}(\#\mathcal{S})$ and Step *b* has complexity $\mathcal{O}(\#R)$. The time complexity for the whole graph transformation/reduction process is therefore $\mathcal{O}(\#R) + \mathcal{O}(\#\mathcal{S})$, which is polynomial. This shows that the problem of interest in this paper is NP-hard and hence a heuristic solution is important.

2.5. The Data Muling Algorithm

In this work, we adapt Dijkstra's algorithm, in the same way it is done in [23], to solve the data muling problem. While many rounds are considered by our algorithm, we consider only the case where each node is visited only once per round. It is assumed that each UAV is capable of collecting and delivering data to a base station where it can be recharged, before going for another data collection round.

Algorithm 1 has two major steps: the first step consists of using Equation 2 to select the best node to visit for every UAV (Step 6-7); the second step consists of adjusting the UAV's paths by choosing the cheapest UAV for every best node (Step 8-23). Once the visitation is done, the collection paths are captured in $Cpaths$ and the two steps are repeated to select the nearest base station for every UAV data delivery following the delivery paths recorded by $Dpaths$.

Algorithm 1: Cooperative algorithm

```
1 Assume a network  $G(N,L,B,P)$  as specified in Section 2.1.2;
2  $Choices \leftarrow$  all sink to be visited ;
3 Initialise the path to the initial hosting base stations;
4  $done \leftarrow choices \cup B$ ;
5 while  $choices \neq \emptyset$  do
6   for  $u \in U$  do
7     | Select the next destination of least cost, using Equation 2 ;
8   end
9    $Assign = \emptyset$ ;
10  for  $u \in U$  do
11    | Let  $c$  be the choice of  $u$ ;
12    for  $v \in U \setminus Assign$  do
13      | if  $u$  and  $v$  selected the same choice  $c$  then
14        | | Include  $c$  in the path of a UAV of least cost (2);
15        | | Include the UAV in  $Assign$ ;
16        | | Include the  $c$  in  $done$ ;
17        | |  $Choices \leftarrow Choices \setminus \{c\}$ ;
18        | | Break;
19      | end
20    end
21    if  $c \in Choices$  then
22      | Include  $c$  in the path of  $u$ ;
23      | Include the  $c$  in  $done$ ;
24      |  $Choices \leftarrow Choices \setminus \{c\}$ ;
25      | Include  $u$  in  $Assign$ ;
26      | Break;
27    end
28  end
29  if  $Choices = \emptyset$  or  $\#done = \#U$  then
30    |  $Choices \leftarrow B$ ;
31    |  $done \leftarrow \emptyset$ ;
32    |  $B \leftarrow \emptyset$ ;
33    | if  $\#done \neq \#U$  then
34      | |  $Cpaths \leftarrow$  all UAVs' paths;
35    | end
36 end
37  $Dpaths \leftarrow$  all current UAVs' paths ;
38 Return  $Cpaths$  and  $Dpaths$ 
```

Proposition 2.6 (Polynomial termination). *Algorithm 1 terminates in polynomial time, when all sink nodes have been visited.*

proof 2.7. *Note that each time a sink is included in a path of one of the UAVs, it gets excluded from the list choice (Lines 16 and 21). Since all UAVs paths consist of a connected graph, whenever choice $\neq \emptyset$, there is at least one UAV which makes a new selection of a next sink to visit on Line 6. So all sink are*

visited.

Once $\text{choice} = \emptyset$, the next destinations become the base stations and the set $\text{done} = \emptyset$ (Lines 25 and 26 consecutively). The next step is to make $\# \text{done} = \#U$ true by assigning to every UAV a base station. In this case the statement at Line 24 is true and the set $\text{choice} = B$ which had been updated to \emptyset . This makes Algorithm 1 stop.

On the other hand, the time complexity of the algorithm is clearly $\mathcal{O}((\#U)^2)$, which is a polynomial. Hence the result follows.

Remark 2.8 (Persistent visitation model). Since each UAV's computed path is ended by a base station and the UAV paths form a static network, Algorithm 1 can be used repetitively to make a persistent visitation.

2.9. Illustration of the algorithm

We illustrate the algorithm in Subsection 1 using an example in Figure 2. We run one round of the algorithm step by step. In this example we consider a case where each sensor node weighting is constantly zero. That is, $\alpha = \beta = 0$ (see the constants in Equation 1).

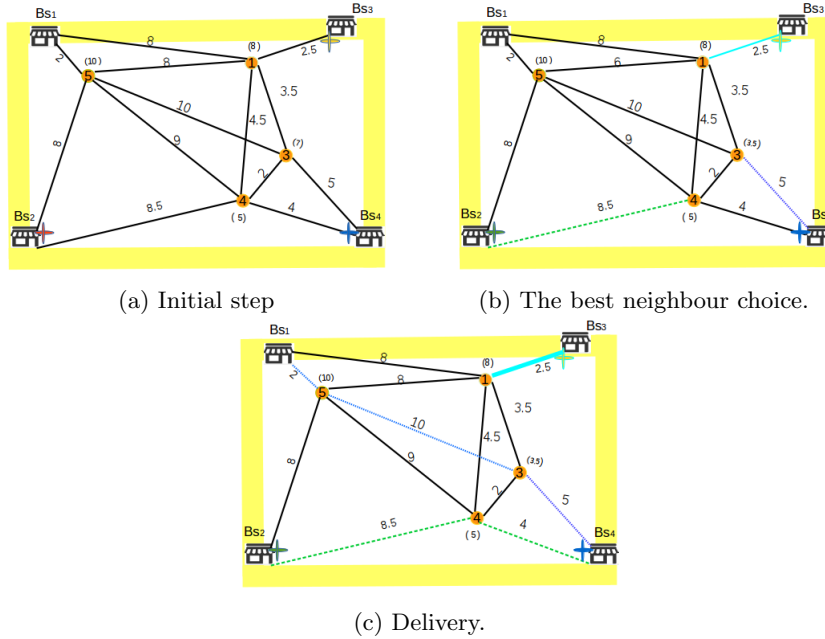


Figure 2: Illustrative example.

Figure 2a shows the initial conditions of the considered system. The system has four sensors, four base stations and three UAVs positioned at all of them except Base station Bs_1 . The links and sensors are weighted as discussed in

Section 2. Let u_2 , u_3 , and u_4 be the name of UAVs staying at Base Stations B_{s_2} , B_{s_3} , and B_{s_4} , respectively.

Figure 2b reveals how the UAVs make choices of their first moves. The best choice is the one corresponding to the cheapest move, which is evaluated using the weight of the road to be used together with the delay at the sensor to be visited. This is why UAVs u_2 , u_3 and u_4 move to Sensors 4, 1 and 3, respectively. At this stage, only node 5 is the only node not yet visited.

Figure 2c shows the next moves up to the end of the algorithm. It shows that UAV u_4 moves to Sensor 5, because it is the one corresponding to the cheapest move. On the other hand, all other UAVs do not have any other choice of sensor to visit. They then need to visit their closest base station. Once UAV u_4 arrives at Node 5, it visits the closest base station which is B_{s_1} .

3. Experimental results

Python was used to run Algorithm 1 on two more complex networks (Figures 3a and 3b). The performance of the algorithm is studied and the behaviours of considered parameters are investigated. The first network (3a) consists of five base stations: B_1 , B_2 , B_3 , B_4 and B_5 , as shown by bigger nodes in Figure 3a. In the figure, smaller nodes represent the sink to be visited and the links in the network show the possible paths, the UAVs may take to visit the targets. Note here that the sink's network (network without base stations) is a complete graph (each UAV is able to move from one sink to any other one in the network, but not to any base station) where nodes are randomly deployed on a $1km^2$ area.

On the other hand, we consider a real network (Figure 3b) consisting of the Cape Town complete network whose nodes are police stations and their Cartesian coordinates have been extracted from GPS positions. The names corresponding to each node label are described in Appendix (see Figures 19a and 19b). Note here that in these experiments the considered UAV are drones.

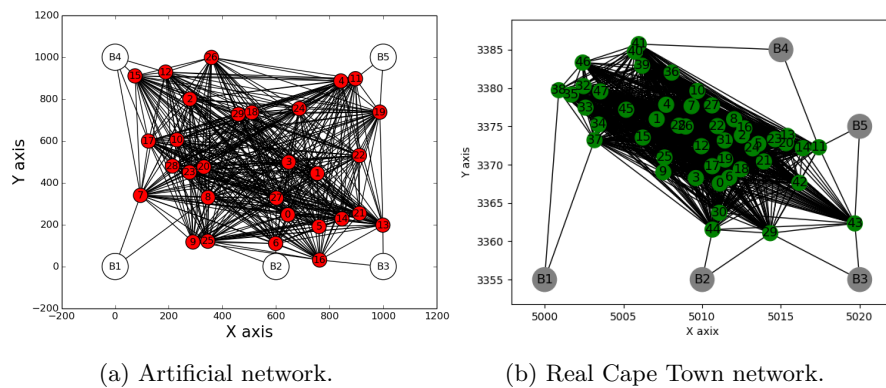
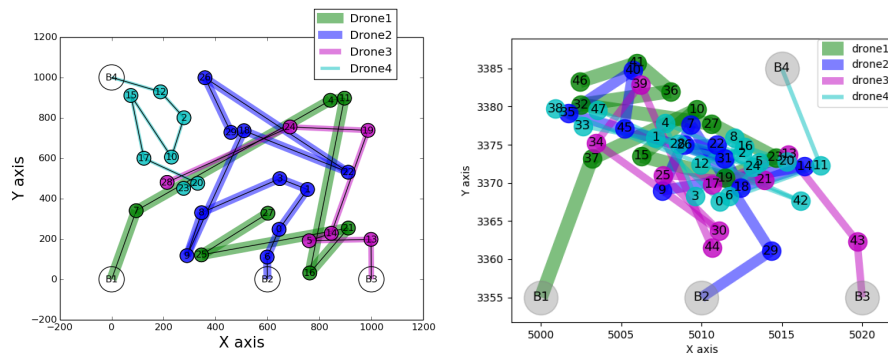


Figure 3: Considered networks.

As shown in Figure 3a, the considered network consists of nodes randomly placed in an area of size $1km^2$ and sinks are labelled in terms of the energy required to collect information from them. The coordinates of nodes in both networks are in metres and could be seen or approximated using Figures 3a and 3b. Positions (of sinks or base stations) consist of triples but for simplicity of plotting/viewing them, they have been projected on X-Y coordinates and hence, they are presented in the 2D Cartesian coordinate system.

3.1. Impact of speed distribution on path planning



(a) Path generation on a random network when the UAVs have the same speed. (b) Path generation on a real network when the UAVs have the same speed.

Figure 4: Path generation.

In two steps, we present the paths taken by UAVs using Algorithm 1.

Step1. Data collection: it consists of visiting all sinks using the first three steps of Algorithm 1. The corresponding path for each UAV is shown in Figures 4a, 4b.

Step2. Data delivery: it consists of visiting base stations using the last step of the same algorithm. The results are shown in Tables 2, 3 and 4, where the speed distribution of drones is also presented.

The assumed cost function parameters are set to $\alpha = \beta = 0.5$ and $\gamma = 1$.

Figures 4a and 4b reveal that UAVs do not visit the same number of sinks in the case of both considered networks. For example in Figure 4a, Drone1, Drone2, Drone3 and Drone4 visit 7, 10, 6 and 7 sinks, respectively.

Table 2 shows that when the speeds are the same for all UAVs, the delivery requires some UAVs to pass by some of the visited nodes to arrive at the base stations. This is because each sinks does not need to be connected at a base station. Table 2a shows that in the case of random network, Drone3 and Drone4 deliver the collected data at the same base station (B_1), and for the real network, Table 2b reveals that Drone1 and Drone4 deliver the data to B4.

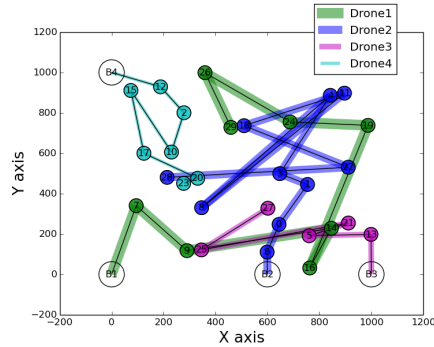
UAV name	Speed(m/min)	Source	Returning path
Drone1	500	B1	[27, 6, B2]
Drone2	500	B2	[29, 12, B4]
Drone3	500	B3	[28, 7, B1]
Drone4	500	B4	[23, 8, B1]

(a) Delivery in the random network.

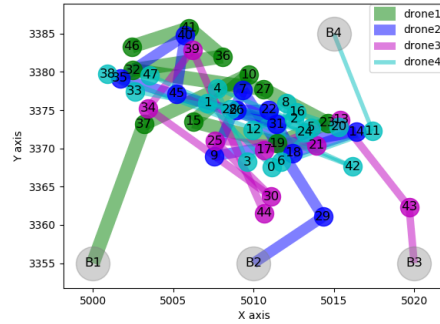
UAV name	Speed(m/min)	Source	Returning path
Drone1	500	B1	[46,41, B4]
Drone2	500	B2	[45, 11, B5]
Drone3	500	B3	[44, B2]
Drone4	500	B4	[47, 12, B4]

(b) Delivery in the real network.

Table 2: Delivery when all speeds are the same.



(a) Paths generation when UAVs have different speeds.



(b) Real network.

Figure 5: Paths generation when the UAVs have the different speeds.

Figure 5 shows that when speeds are different, some UAVs may not change their paths but other not. For example Drone4 does not change its path in both Figures 5a and 5b, whereas all other drones do. On the other hand Figure 5b shows that for the real network, all drones keep their paths.

UAV name	Speed(m/min)	Source	Returning path
Drone1	800	B1	[29, 12, B4]
Drone2	700	B2	[28, 7, B1]
Drone3	600	B3	[27, 6, B2]
Drone4	500	B4	[23, 8, B1]

(a) Random network.

UAV name	Speed(m/min)	Source	Returning path
Drone1	800	B1	[46,41, B4]
Drone2	700	B2	[45, 11, B5]
Drone3	600	B3	[44, B2]
Drone4	500	B4	[47, 12, B4]

(b) Real network.

Table 3: Data delivery when all drones have the different speed.

Table 3 shows that when the speeds are different, the delivery also requires some UAVs to pass by some of the already visited nodes, in order to arrive at a closest base stations. Table 3a shows that Drone2 and Drone4 deliver the collected data at the same base station (B_1), and Table 3b shows that Drone1 and Drone4 deliver the collected data at the same base station (B_4).

It is shown in Figure 6, that the distribution of the UAVs speeds, have an impact on paths generation. For example Figure 6a shows that Drone1, Drone2,

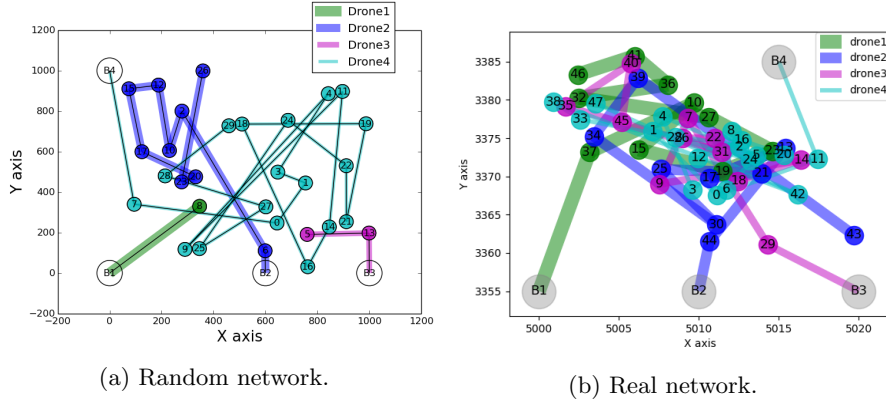


Figure 6: Paths generation when speeds distribution is changed.

Drone3 and Drone4 visit 1, 9, 2 and 18 sink, respectively. This shows a big difference due to the fact that the choice of target depends on the current and not the previous visitation costs, together with the change of speed distribution in base stations.

UAV name	speed (m/min)	Source	Returning path
Drone1	500	B1	[8, 6, B2]
Drone2	600	B2	[26, 12, B4]
Drone3	700	B3	[5, 16, B3]
Drone4	800	B4	[29, 15, B4]

(a) Random network.

UAV name	Speed(m/min)	Source	Returning path
Drone1	500	B1	[46,41, B4]
Drone2	600	B2	[43, B3]
Drone3	700	B3	[45, 11, B5]
Drone4	800	B4	[47, 12, B4]

(b) Real network.

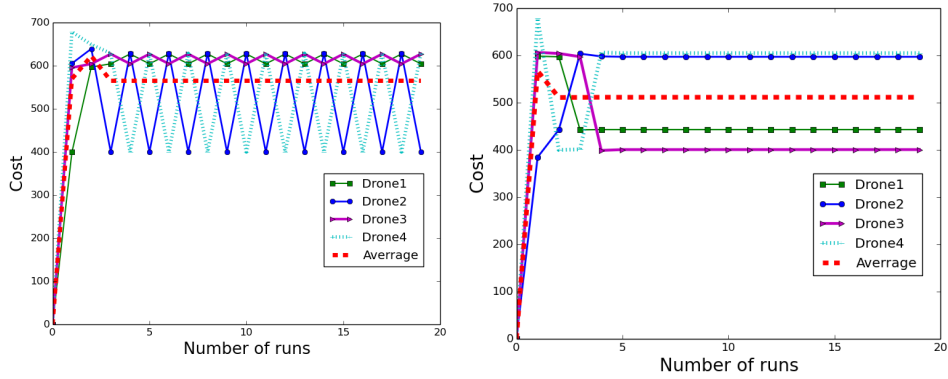
Table 4: Data delivery when speed distribution changes.

Table 4 shows that when the speeds are differently distributed, the paths are changed and thus the delivery paths also change. Table 4a shows that for the random network, Drone2 and Drone4 deliver the collected data at the same base station (B_4); and for the real network, Table 4b shows that Drone1 and Drone4 deliver the collected data at the same base station (B_4)

Since the path generation for both network essentially behave the same, we consider (the artificial) random network for the next analysis.

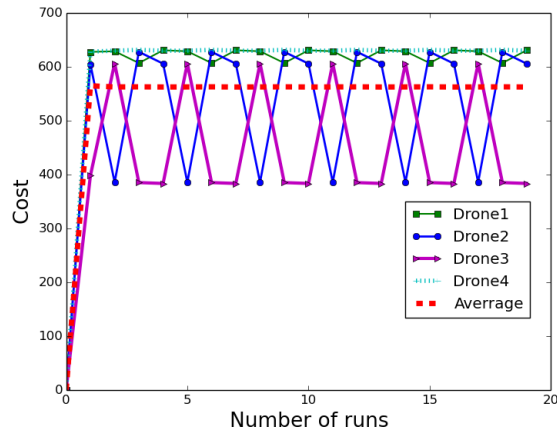
3.2. Impact of the speed distribution on the cost (total energy)

We now study the impact of speed distribution on the cost considering many runs of the algorithm. We perform 20 runs of Algorithm 1 in three cases of speed distribution, as shown by the second columns, in Tables 2, 3 and 4. Figure 7a shows a case where each UAV's speed equals 500m/min, and on the other side Figure 7b corresponds to the case where UAVs have different speeds as shown in Table 2.



(a) Cost at same speed.

(b) Cost at different UAVs' speeds.



(c) Cost related to a different speed distribution.

Figure 7: Impact of speed distribution.

Figure 7a reveals that the cost for each drone lies in one of few fixed values. Drone4 takes four values and all others take three and succeed each other to take the minimum and maximum values. The average cost is constantly close to 560.

Figure 7b shows that after the first four runs, all UAVs correspond to constant costs where the average cost is constantly close to 500.

Figure 7c shows that the change in speed distribution may change the average cost and also the trends of the cost function. In this case, the amended speed distribution corresponds to the one in Table 4, and shows that for each UAV, the cost changes periodically and can only take one of a few fixed values. This is why the average cost also takes one of the fixed values on a periodic basis.

3.3. Effect of parameters variation

In this subsection, we study the effect of four parameters on the cost variation as the number of runs varies. The four considered parameters are described as follows.

- **Speed value:** keeping the speed the same for all UAVs, we aim to study the impact of its increase on the coverage cost.
- **Overdue time (α).** we study the impact of overdue time on the cost. Great attention is placed on this time by incrementing the corresponding coefficient (penalty) by 0.05, for each new run.
- **Delay (β).** While all the other parameters are constant, We vary the parameter corresponding to the delay penalty and study how it changes the value of the coverage cost.
- **Data collection rate (γ).** Data collection rate is incremented by 0.05 for its value $\gamma = 1$, of 20 runs of the algorithm.

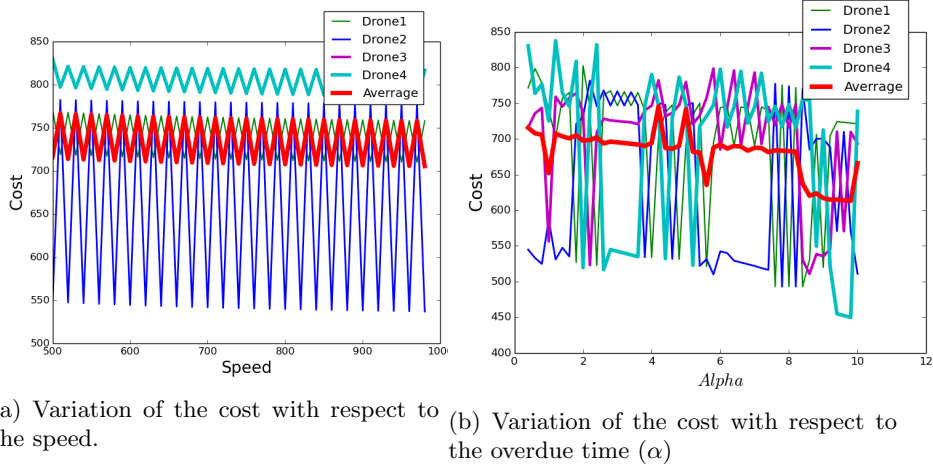
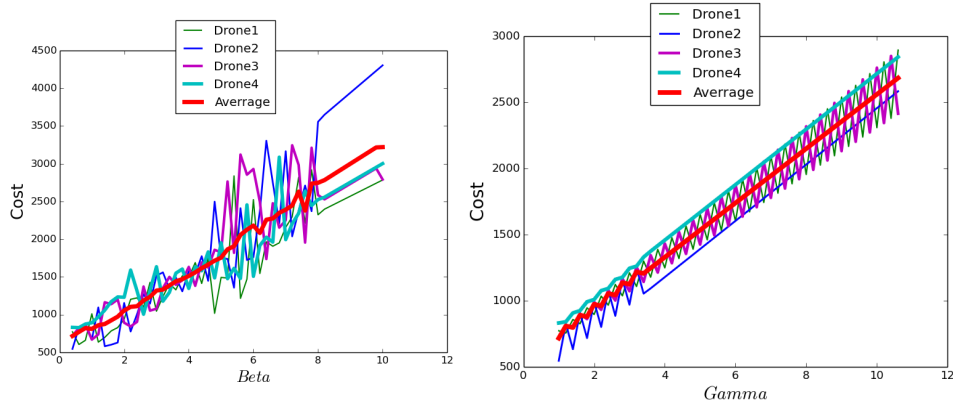


Figure 8: Impact of Speed and overdue time on the total cost.

Figure 8a shows a case where the speed has been incremented 20 times for all UAVs. It shows that from the first run, each UAV periodically changes its cost between two cost values. Drone4 corresponds to the highest cost while notably Drone3 corresponds exactly to the average cost.

Figure 8b shows a case where the overdue time (α) is incremented by 0.5, at each of 20 consecutive runs. The values of cost corresponding to each UAV is stochastic and the average is stochastically decreasing.

We consider a case where the latency is the factor that changes in Figure 18c. The figure shows stochastic values as well but however the average cost is mostly increasing.



(a) Variation of the cost with respect to the delay (β) (b) Variation of the cost with respect to the data collection rate.

Figure 9: Impact of the delay and data collection rate on the total cost.

Figure 9b shows the impact of γ on the variation of the cost over 20 runs. It shows that Drone4 mostly corresponds to the highest cost, and once $\gamma > 3.8$, Drone4 and Drone2 are constantly increasing their corresponding costs, whereas the others are periodically increasing and decreasing.

3.4. Prioritisation analysis

In this subsection, we discuss the effect of the delay and overdue time boundaries. We assume the same network as shown by Figure 3a, where the UAVs *drone1*, *drone2* and *drone3* are initially positioned at Base Stations *B1*, *B2* and *B3*, respectively; and all the UAVs are assumed to have the same speed $v=800$ m/min.

3.4.1. Effect of delay constraints on path design

Figure 10 and Table 5 represent the case where, each sensor node is visited if the arrival of a drone is late for no more than 30 min.

Figure 10 shows that 14 sensor nodes could not be visited (see red hexagon shaped nodes). The UAV *drone3* visits most of the visited nodes, whereas other UAVs could visit only 3 sensors each. Table 5 shows that Drone1 delivers to Base Station *B4* via node 12, Drone2 to Base Station *B3* via node 14 and then 13 and Drone3 to Base station *B3* via node 16.

Table 6 shows the data delivery paths when UAVs may be late no more than 60 min, and Figure 11 shows the data collection path with this setting.

When changing the late threshold to 60 min, Table 6 shows that the delivery paths changed, and the delivery is done as the last column of the table shows.

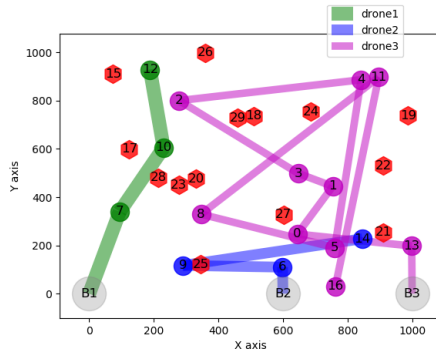


Figure 10: Paths details (waiting=30).

UAV name	speed (m/min)	Source	Returning path
Drone1	800	B1	[12, B4]
Drone2	800	B2	[14, 13, B3]
Drone3	800	B3	[16, B3]

Table 5: Data delivery when UAVs may be late for no more than 30 min.

Comparing with Figure 10, Figure 11 reveals that *drone3* does not change the path, but the other UAVs extend their path to two more sensor nodes each. This results in 10 sensor nodes to be missed as shown by the figure.

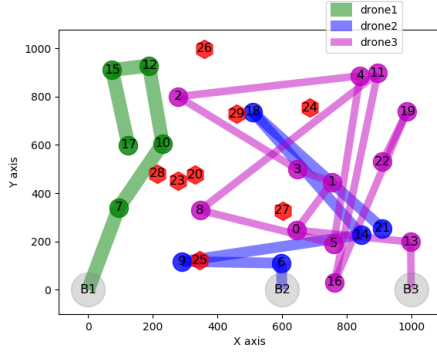


Figure 11: Paths details (waiting=60).

UAV name	speed (m/min)	Source	Returning path
Drone1	800	B1	[17, B4]
Drone2	800	B2	[21, 13, B3]
Drone3	800	B3	[22, 19, B5]

Table 6: Data delivery when UAVs may be late for no more than 60 min.

Table 7 and Figure 12 respectively show the data delivery and collection paths, when UAVs may be late for a very long time.

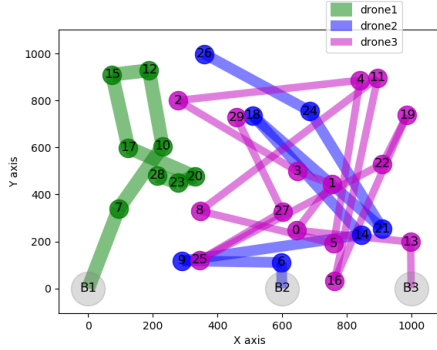


Figure 12: Paths details (waiting= ∞).

UAV name	speed (m/min)	Source	Returning path
Drone1	800	B1	[28, 7, B1]
Drone2	800	B2	[26, 12, B4]
Drone3	800	B3	[29, 15, B4]

Table 7: Data delivery when UAVs may be late for no more than 60 min.

Comparing with the previous two cases, Table 7 shows that the delivery paths keep on changing different.

Figure 12 shows that all nodes have been visited and the path of each drone has been extended, to cover more nodes.

Figure 13 reveals the changes in the number of missed nodes while the late threshold evolves. The figure shows that when the delay threshold increases, the number of unvisited nodes remains constant or decreases (it does never increase), until it converges to zero. This is justified by the fact that, allowing a longer delay increases the chance for a node to be visited.

3.4.2. Effect of overdue constraints on path design

In this section, we study the effect of the waiting constraints. Here, sensors can only be visited after some fixed time called the waiting threshold.

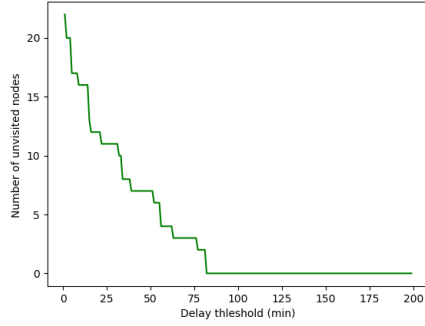
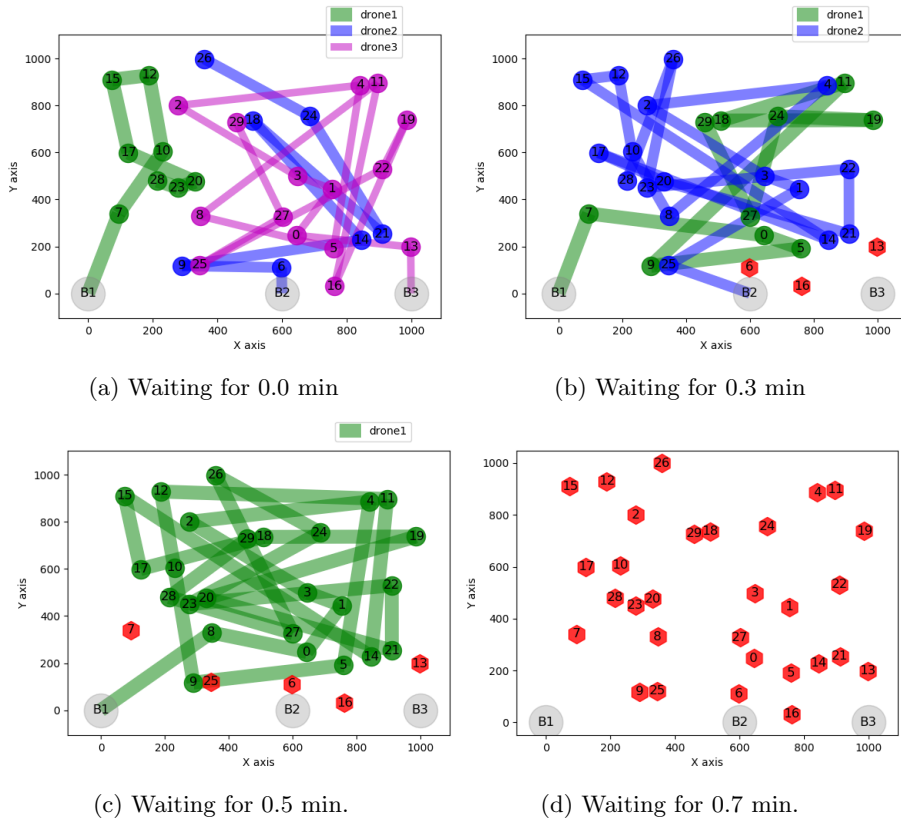


Figure 13: Number of unvisited nodes.



(a) Waiting for 0.0 min

(b) Waiting for 0.3 min

(c) Waiting for 0.5 min.

(d) Waiting for 0.7 min.

Figure 14: Visitation constrained by the waiting time.

Figure 14 shows how paths corresponding to different thresholds are generated. Figure 14a considers a case where there is no waiting limitation (waiting

time is zero) and clearly all sensors are visited. When the waiting time is set to 0.3 minutes (18 seconds) in Figure 14b three nodes are not visited and the Drone 3 could not visit any sensor. Setting the waiting threshold to 0.5 min, only UAV Drone 1 could visit and 5 sensors were missed. Setting the waiting time to 0.7 min, no node could be visited. This is because there is a specific time for UAVs to arrive at each sensors which depend on the distance and speed. If the distance is small and the UAV can arrive earlier than the waiting threshold, the visitation is impossible.

UAV name	speed (m/min)	Source	Returning path
Drone1	800	B1	[28, 7, B1]
Drone2	800	B2	[26, 12, B4]
Drone3	800	B3	[29, 15, B4]

(a) Data delivery when the waiting threshold is 0 min.

UAV name	speed (m/min)	Source	Returning path
Drone1	800	B1	[29, 12, B4]
Drone2	800	B2	[28, 7, B1]
Drone3	800	B3	[B3]

(b) Data delivery when the waiting threshold is 0.3 min.

Table 8: Data delivery when the waiting threshold is small.

UAV name	speed (m/min)	Source	Returning path
Drone1	800	B1	[29, 12, B4]
Drone2	800	B2	[B2]
Drone3	800	B3	[B3]

(a) Data delivery when the waiting threshold is 0.5 min.

UAV name	speed (m/min)	Source	Returning path
Drone1	800	B1	[B1]
Drone2	800	B2	[B2]
Drone3	800	B3	[B3]

(b) Data delivery when the waiting threshold is 0.7 min.

Table 9: Data delivery when the waiting threshold is high.

Tables 9 and 8, show deliveries corresponding to visitations shown in Figure 14. Note that if a UAV does not visit any sensor, it remains at its initial position.

Keeping on changing the waiting threshold, Figure 15 shows the corresponding number of missed sensors.

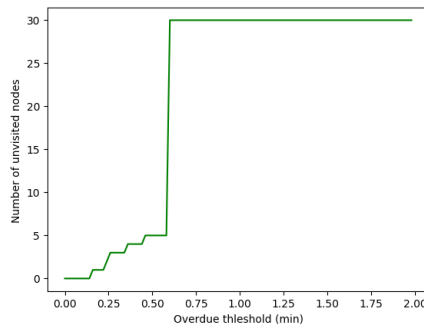


Figure 15: Number of unvisited nodes.

Figure 15 reveals that the number of missed nodes increases as the waiting threshold increases and converges to the total number of sensors to be visited.

3.4.3. Persistent visitation analysis

In this subsection, we study the trend of paths while UAVs persistently visit sensors. Persistent visitation is done by resetting the initial base stations for the next visit, to the destination of the previous visitation.

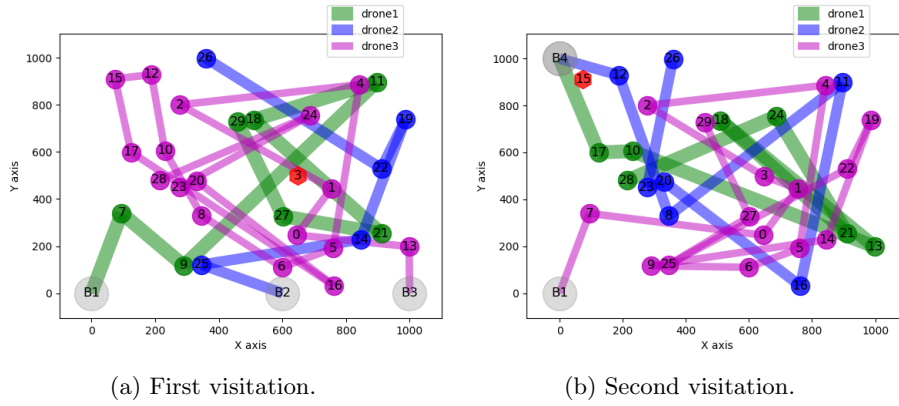


Figure 16: First two visitations.

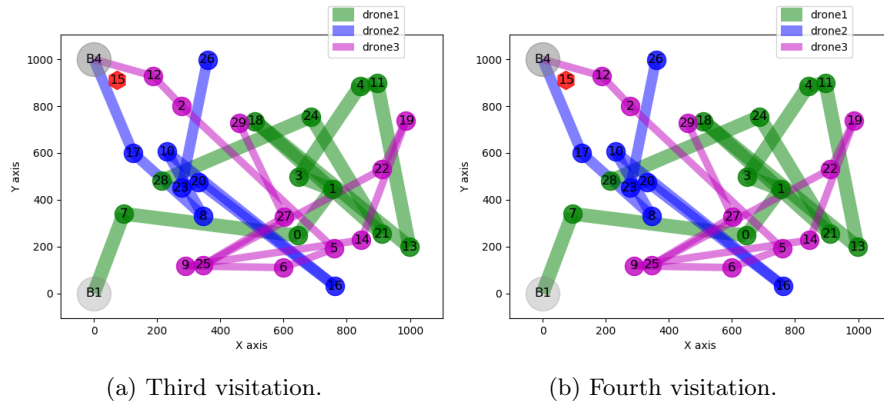
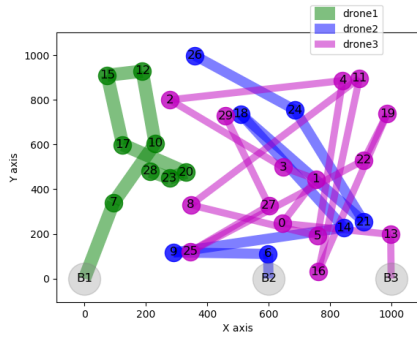


Figure 17: Next two visitations.

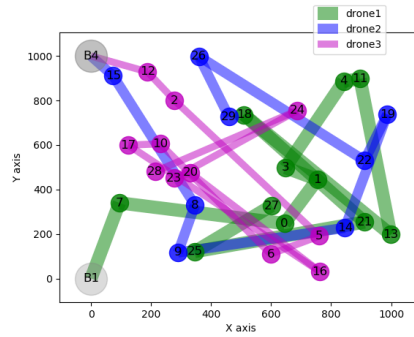
Figure 17 shows four consecutive visitations and deliveries when the waiting threshold is set to 12 seconds. Figure 16a shows that only node 3 has not been visited. Figure 16b shows that a new node (node 15) has not been visited and all visitation paths change. Figure 17a shows that paths keep on changing and non-visited nodes remain the same as the previous visitation.

Note that Figure 17b is exactly the same as Figure 17a. This shows that all the following paths will be the same as Figure 17a and hence paths generation may converge to specific paths. This is a special case where UAVs' initial positions become the same as their optimal destination.

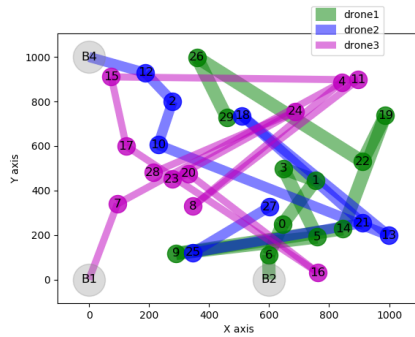
We now consider the constraint free visitations and study the pattern of generated paths.



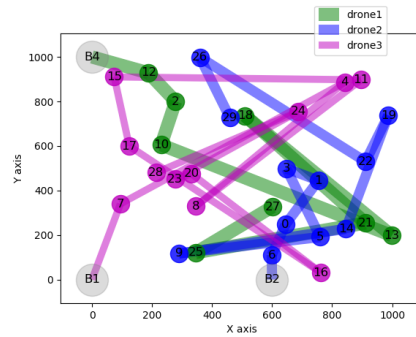
(a) First visitation



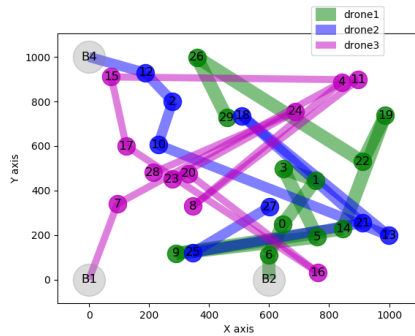
(b) Second visitation.



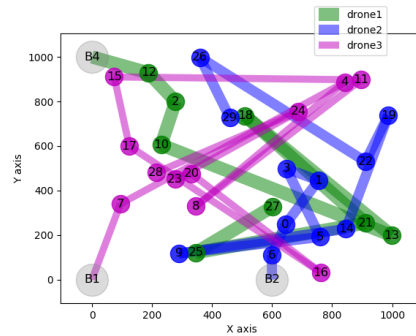
(c) Third visitation.



(d) Fourth visitation.



(e) sixth visitation.



(f) seventh visitation.

Figures 18a, 18b, 18c, 18d, 18e, 18f show the first 6 consecutive unconstrained visitations. The path change and from the third visitation, paths generation becomes periodic: third visitation is same as the fifth, and the fourth visitation is the same as the sixth. This shows that after each next visitations

paths generation remains the same. This is justified by the fact that from each base station, each UAV has a single optimal destination.

4. Conclusion and future work

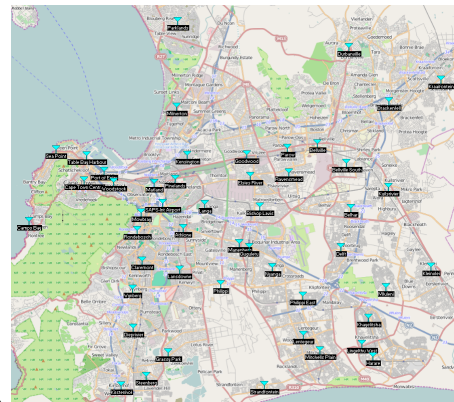
In this paper, a model for data muling targeting revisit costs minimization for a team of UAVs has been provided. A mathematical formulation of the model has been presented and the underlying problem has been polynomially reduced to another NP-hard problem and hence proved to be an NP-hard problem. A heuristic solution to the problem has been provided and its performance evaluated through simulation experiments. Simulation results have revealed different path distribution patterns under different experimental settings and the impact of these settings on path length fairness and related energy cost. Furthermore, simulations show that consecutive paths generation becomes periodic after some number of visitations. While this paper has presented the basis of a data muling model aiming at supplementing traditional traffic engineering techniques used in sink networks, several network and traffic aspects related to the proposed data muling model still need to be investigated. These include the design of efficient communication models that consider the outdoor characteristics of drone-to-sink communication as suggested in [27]. Taking advantage of the emerging white space frequency bands as discussed in [28] to achieve drone-to-sink and drone-to-drone communication is another direction for further work.

5. Appendix

We assume the public safety network consisting of Cape Town (South Africa) police stations as collection points of a ground sensor network used for example for city safety or traffic control. Cape Town police stations are labelled in terms of integers in interval $[1, 49]$ and their GPS coordinates are used as their positions (see Figure 19a). The corresponding positions on a map are shown in Figure 19b.

Label	Station	Longitude	Latitude
1.	Bellville	33°54'06"S	018°37'12"E
2.	Nyanga	33°59'20"S	018°34'54"E
3.	SAPS-Int Airport	33°56'37"S	018°29'18"E
4.	Bellville South	33°54'55"S	018°38'40"E
5.	Philippi	34°00'02"S	018°32'16"E
6.	Matland	33°55'46"S	018°28'52"E
7.	Parow	33°54'16"S	018°35'39"E
8.	Lansdowne	33°59'26"S	018°30'10"E
9.	Rondebosch	33°57'46"S	018°27'59"E
10.	Kuilsrivier	33°55'56"S	018°40'50"E
11.	Wynberg	34°00'15"S	018°27'46"E
12.	Sea Point	33°54'20"S	018°23'51"E
13.	Bishop Lavis	33°56'46"S	018°34'15"E
14.	Cape Town Central	33°55'40"S	018°25'16"E
15.	Table Bay Harbour	33°54'38"S	018°25'24"E
16.	Deift	33°58'29"S	018°38'24"E
17.	Mowbray	33°57'00"S	018°28'12"E
18.	Ravenshead	33°55'13"S	018°35'45"E
19.	Goodwood	33°54'33"S	018°33'35"E
20.	Elsies River	33°55'28"S	018°33'46"E
21.	Port of Entry	33°55'15"S	018°26'18"E
22.	Kensington	33°54'34"S	018°30'33"E
23.	Athlone	33°57'41"S	018°30'20"E
24.	Woodstock	33°55'43"S	018°26'48"E
25.	Pinelands	33°55'36"S	018°29'56"E
26.	Belhar	33°56'49"S	018°38'55"E
27.	Manenberg	33°58'18"S	018°33'13"E
28.	Claremont	33°59'04"S	018°28'15"E
29.	Guguletu	33°58'29"S	018°33'43"E
30.	Durbanville	33°50'01"S	018°38'40"E
31.	Brackenfell	33°52'18"S	018°40'51"E
32.	Langa	33°56'39"S	018°31'27"E
33.	Mitchells Plain	34°02'52"S	018°27'19"E
34.	Khayelitsha	34°01'29"S	018°39'48"E
35.	Mfuleni	34°00'11"S	018°40'43"E
36.	Lingelthu West	34°02'35"S	018°30'28"E
37.	Dieprivier	34°01'64"S	018°27'47"E
38.	Kleinvllei	33°59'18"S	018°43'00"E
39.	Harare	34°03'06"S	018°40'01"E
40.	Grassy Park	34°02'55"S	018°29'35"E
41.	Steenberg	34°03'56"S	018°28'28"E
42.	Kirstenhof	34°04'19"S	018°27'11"E
43.	Camps Bay	33°57'22"S	018°22'29"E
44.	Milnerton	33°52'32"S	018°30'01"E
45.	Parklands	33°48'55"S	018°38'04"E
46.	Kraaifontein	33°51'24"S	018°18'30"E
47.	Philippi East	34°00'32"S	018°36'27"E
48.	Strandfontein	34°04'19"S	018°34'29"E
49.	Lentegeur	34°02'11"S	018°36'29"E

(a) GPS positions of Cape Town police stations.



(b) Positions on the globe's map.

Figure 19: Raw real network study.

References

- [1] A. Bagula, L. Castelli, M. Zennaro, On the design of smart parking networks in the smart cities: An optimal sensor placement model, *Sensors* 15 (7) (2015) 15443–15467 (2015).
- [2] A. Bagula, M. Zennaro, G. Inggs, S. Scott, D. Gascon, Ubiquitous sensor networking for development (usn4d): An application to pollution monitoring, *Sensors* ISSN 1424-8220 12 (7) (2012) 391–414 (2012).
- [3] M. Masinde, A. Bagula, A framework for predicting droughts in developing countries using sensor networks and mobile phones, in: *Proceedings of the 2010 Annual Research Conference of the South African Institute of Computer Scientists and Information Technologists*, ACM, 2010, pp. 390–393 (2010).
- [4] M. Masinde, A. Bagula, T. N. Mthama, The role of icts in downscaling and up-scaling integrated weather forecasts for farmers in sub-saharan africa, in: *In proceedings of ICTD'12*, ACM, 2012, pp. 122–129 (2012).

- [5] M. Mandava, C. Lubamba, A. Ismail, H. Bagula, A. Bagula, Cyber-healthcare for public healthcare in the developing world, in: Proceedings of the 2016 IEEE Symposium on Computers and Communication (ISCC), IEE, 2016, pp. 14–19 (2016).
- [6] A. Bagula, C. Lubamba, M. Mandava, A. Ismail, H. Bagula, , M. Zenaro, E. Pietrosemoli, Cloud based patient prioritization as service in public health care, in: Proceedings of the ITU Kaleidoscope 2016, Bangkok, Thailand, 14-16 November, IEE, 2016 (2016).
- [7] J. Las Fargeas, B. Hyun, P. Kabamba, A. Girard, Persistent visitation with fuel constraints, *Procedia-Social and Behavioral Sciences* 54 (2012) 1037–1046 (2012).
- [8] J. Las Fargeas, B. Hyun, P. Kabamba, A. Girard, Persistent visitation under revisit constraints, in: *Unmanned Aircraft Systems (ICUAS), 2013 International Conference on*, IEEE, 2013, pp. 952–957 (2013).
- [9] J. Las Fargeas, P. Kabamba, A. Girard, Cooperative surveillance and pursuit using unmanned aerial vehicles and unattended ground sensors, *Sensors* 15 (1) (2015) 1365–1388 (2015).
- [10] J. Las Fargeas, P. Kabamba, A. Girard, Optimal configuration of alarm sensors for monitoring mobile ergodic markov phenomena on arbitrary graphs (2015).
- [11] E. Tuyishimire, I. Adiel, S. Rekhis, B. A. Bagula, N. Boudriga, Internet-of-things in motion: A cooperative data muling model under revisit constraints, in: proceedings of the 13th IEEE International Conference on Ubiquitous Intelligence and Computing, presented on 2016 July, 18-21 Toulouse, France.
- [12] A. Bagula, E. Tuyishimire, J. Wadepoel, N. Boudriga, S. Rekhis, Internet-of-things in motion: A cooperative data muling model for public safety, in: proceedings of the 13th IEEE International Conference on Ubiquitous Intelligence and Computing, presented on 2016 July, 18-21 Toulouse, France.
- [13] M. A. Bender, S. P. Fekete, A. Kröller, V. Liberatore, J. S. Mitchell, V. Polishchuk, J. Suomela, The minimum backlog problem, *Theoretical Computer Science* 605 (2015) 51–61 (2015).
- [14] G. Citovsky, J. Gao, J. S. Mitchell, J. Zeng, Exact and approximation algorithms for data mule scheduling in a sensor network, in: *International Symposium on Algorithms and Experiments for Sensor Systems, Wireless Networks and Distributed Robotics*, Springer, 2015, pp. 57–70 (2015).
- [15] E. Tuyishimire, A. Bagula, A. Ismail, Clustered data muling in the internet of things in motion, *Sensors* 19 (3) (2019) 484 (2019).

- [16] A. Ismail, B. Bagula, E. Tuyishimire, Internet-of-things in motion: A uav coalition model for remote sensing in smart cities, *Sensors* 18 (7) (2018) 2184 (2018).
- [17] E. Tuyishimire, B. A. Bagula, A. Ismail, Optimal clustering for efficient data muling in the internet-of-things in motion, in: *International Symposium on Ubiquitous Networking*, Springer, 2018, pp. 359–371 (2018).
- [18] A. Ismail, E. Tuyishimire, A. Bagula, Generating dubins path for fixed wing uavs in search missions, in: *International Symposium on Ubiquitous Networking*, Springer, 2018, pp. 347–358 (2018).
- [19] E. Tuyishimire, A. Bagula, S. Rekhis, N. Boudriga, Cooperative data muling from ground sensors to base stations using uavs, in: *2017 IEEE Symposium on Computers and Communications (ISCC)*, IEEE, 2017, pp. 35–41 (2017).
- [20] E. Tuyishimire, B. A. Bagula, J. Sanders, Internet of things: Least interference beaconing algorithms, Ph.D. thesis, University of Cape Town (2014).
- [21] E. T. T. N. Hope Mauwa, Antoine Bagula, An optimal spectrum allocation strategy for dynamic spectrum markets, in: *International Conference on Wireless and Mobile Computing, Networking and Communications*, IEEE, 2019 (2019).
- [22] E. T. T. N. Hope Mauwa, Antoine Bagula, Community healthcare mesh network engineering in white space frequencies, in: *ITU ACADEMIC CONFERENCE*, IEEE, 2019 (2019).
- [23] A. Pal, N. Memon, The evolution of file carving, *Signal Processing Magazine*, IEEE 26 (2) (2009) 59–71 (2009).
- [24] E. W. Dijkstra, A note on two problems in connexion with graphs, *Numerische matematik* 1 (1) (1959) 269–271 (1959).
- [25] G. Laporte, The vehicle routing problem: An overview of exact and approximate algorithms, *European Journal of Operational Research* 59 (3) (1992) 345–358 (1992).
- [26] P. Toth, D. Vigo, An overview of vehicle routing problems, in: *The vehicle routing problem*, Society for Industrial and Applied Mathematics, 2001, pp. 1–26 (2001).
- [27] M. Zennaro, H. Ntareme, A. Bagula, Experimental evaluation of temporal and energy characteristics of an outdoor sensor network, in: *Proceedings of the International Conference on Mobile Technology, Applications, and Systems*, Article 99, ACM, 2008 (2008).

- [28] T. X. Brown, E. Pietrosevoli, M. Zennaro, A. Bagula, H. Mauwa, S. M. Nleya, A survey of tv white space measurements in e-infrastructure and e-services for developing countries,, 2015, pp 164-172., in: Lecture Notes of the Institute for Computer Sciences, Social Informatics and Telecommunications Engineering, Volume 147, EAI, 2015, pp. 164–172 (2015).